IMPACT OF SOIL WATER CONTENT ON LANDMINE DETECTION USING RADAR AND THERMAL INFRARED SENSORS

Sung-ho Hong, Tim Miller, Harold Tobin, Brian Borchers, and Jan M.H. Hendrickx
New Mexico Tech, Socorro, NM 87801
hendrick@nmt.edu

Henk Lensen and Piet Schwering
TNO-FEL, The Hague, The Netherlands

Brian Baertlein
The Ohio State University, Columbus OH

ABSTRACT

Land mines are a major problem in many areas of the world. In spite of the fact that many different types of land mines sensors have been developed, the detection of non-metallic land mines remains very difficult. Most landmine detection sensors are affected by soil properties such as water content, temperature, electrical conductivity and dielectric constant. The most important of these is water content since it directly influences the three other properties. In this study, the ground penetrating radar and thermal infrared sensors were used to identify non-metallic landmines in different soil and water content conditions.

Keywords: Landmine Detection, Ground Penetrating Radar, Thermal Infrared Sensor, Dielectric Properties

1. INTRODUCTION

The detection and disposal of anti-personnel and anti-tank landmines is one of the most difficult and uncontrollable problems faced in ground conflict. Since mines remain lethal long after military actions have terminated, they also have become a humanitarian disaster. Today at least 100 million landmines are scattered across more than 60 countries. Unfortunately, no perfect landmine detection technique is currently available. One reason is that sensor developers often have not taken into account the effect of soil moisture regimes in different soils and different climates on land mine detection by ground penetrating radar and thermal infrared sensors.[1,2,3,4,5]

Two types of sensors have shown great potential for detecting landmines under various environmental conditions: microwave radar and infrared imaging sensors. These mine detection sensors are affected by soil properties such as water content, temperature, electrical conductivity and dielectric constant. The most important of these is water content since it directly influences the three other properties. Previous work has focused on the modeling of the effect of soil water content changes on mine signatures obtained with radar and thermal infrared sensors.

The objective of this study is to conduct field experiments at Socorro, New Mexico, to measure the impact of soil water content changes on mine detection using ground penetrating radar and thermal infrared sensors. The measurements will be used to validate our modeling results and to define optimal environmental conditions to use these sensors.

2. MODEL OF RADAR RESPONSE

The radar response from a soil and land mine depend on a number of soil properties such as bulk density, specific density of the soil particles, texture, volumetric water content, temperature, and radar frequency. Using a collection of models from the literature we can determine whether or not field conditions are suitable for use of GPR for detection of an antitank mine.[3] As a GPR signal travels through the soil, it is attenuated at a rate determined by the complex dielectric constant of the soil. The round trip attenuation loss (*AL*) is given by

$$\text{Attenuation Loss} = 17.3718\, \mathrm{d}\, \alpha \tag{1}$$

where *d* is the depth to the object from which the GPR signal is reflecting and α is

$$\alpha = \frac{2\pi f}{c} \sqrt{\frac{\varepsilon_{s'}}{2}\left(\sqrt{1+\left(\frac{\varepsilon_{s'}}{\varepsilon_{s''}}\right)^{2}} - 1\right)} \tag{2}$$

where

$$\varepsilon_{s'} = 1.15\left[1 + \frac{\rho_{\mathrm{B}}}{\rho_{\mathrm{S}}}\left(\varepsilon_{\mathrm{p}}^{\alpha} - 1\right) + \theta^{\beta'}\, \varepsilon'^{\alpha}_{\mathrm{fw}} - \theta\right]^{1/\alpha} - 0.68 \tag{3}$$

and

$$\varepsilon_{\mathrm{s}}'' = \left[\theta^{\beta''}\, \varepsilon''^{\alpha}_{\mathrm{fw}}\right]^{1/\alpha} \tag{4}$$

where ρ_{B} is the density of the soil particles, ρ_{S} is the bulk density of the soil, ε_p is the dielectric constant of soil particles, ε_s is the dielectric constant of bulk soil, θ is the volumetric water content, *f* is the frequency, ε_{fw} is the dielectric constant of free water and α is a constant (0.65).

$$\beta' = 127.48 - 0.519\, S - 0.152\, C \tag{5}$$

$$\beta'' = 1.33797 - 0.603\, S - 0.166\, C \tag{6}$$

where *S* is the fraction of sand particles and *C* is the fraction of the clay particles.

$$\varepsilon_{\mathrm{fw}}'' = \frac{2\pi\, \mathrm{f}\, \tau_{\mathrm{w}}\left(\varepsilon_{\mathrm{w}0} - \varepsilon_{\mathrm{w}\infty}\right)}{1 + (2\pi\, \mathrm{f}\, \tau_{\mathrm{w}})^{2}} + \frac{\sigma_{\mathrm{eff}}}{2\pi\, \varepsilon_0\, \mathrm{f}} \frac{(\rho_{\mathrm{S}} - \rho_{\mathrm{B}})}{\rho_{\mathrm{S}}\, \theta} \tag{7}$$

$$\varepsilon_{\mathrm{f'w}} = \varepsilon_{\mathrm{w}\infty} + \frac{\varepsilon_{\mathrm{w}0} - \varepsilon_{\mathrm{w}\infty}}{1 + (2\pi\, \mathrm{f}\, \tau_{\mathrm{w}})^{2}} \tag{8}$$

where ε_0 is the dielectric permittivity of free space, $\varepsilon_{\mathrm{w}0}$ is the static dielectric constant of water, $\varepsilon_{\mathrm{w}\infty}$ is the high frequency limit of $\varepsilon_{\mathrm{f'w}}$, and τ_{w} is the relaxation time of water.

A second factor that determines the performance of the GPR for land mine detection is the strength of signal reflection when it reflects back from the landmine. The reflection loss (*RL*) is given by

$$\text{Reflection Loss} = -10 \log |\mathrm{r}|^{2} \tag{9}$$

where

$$r = \frac{\sqrt{\varepsilon_s} - \sqrt{\varepsilon_m}}{\sqrt{\varepsilon_s} + \sqrt{\varepsilon_m}} \tag{10}$$

where ε_s is the dielectric constant for the bulk soil, and ε_m is the dielectric constant of mine.

The reflection coefficient depends on the difference between dielectric constants of the mine and the soil. As these constants approach each other, the strength of the reflected wave goes to zero, and the mine becomes invisible.

The mathematical models described here have been integrated into a MATLAB package that can be used to predict the performance of ground penetrating radar systems under field conditions. The necessary input data consists of the soil texture (in the form of sand and clay fractions), the bulk soil density, and the volumetric soil water content.

3. THERMAL SIGNATURE OF LANDMINE

DePersia et al.[6] reported on thermal signatures in areas with land mines. They pointed out that the localized thermal variances of the soil are generated by the buried landmines because landmines impact the soil moisture distribution and heat capacity as well as cause a surface disturbance during burring the mine. The major principle of thermal infrared sensors for mine detection is based on detecting localized temperature differences introduced by the mines.

4. METHODS AND MATERIALS

Study Site
Two study sites were located in the Sevilleta National Wildlife Refuge near Socorro NM. A sand site was located near the Rio Salado sand dunes. The sand had a composition of 95% sand and 5% clay. The silt site was located close to the Rio Salado. The soil was classified as a silt loam with a composition of 10% sand, 15% clay, and 75% silt. At each of these sites we buried an antitank mine (Figure 1). During dry, intermediate and saturated field conditions, thermal images, GPR profiles , and water content profiles were recorded.

Figure 1: Inert Antitank Mine (0.3 m diameter)

Equipment
We used a ground penetrating radar (pulseEKKO 1000) system manufactured by Sensors and Software Ltd, Canada. We chose the 900 MHz antenna with an antenna separation of 0.170 cm. For data collection we used a step size of 2.5 cm, reflection mode survey type, and 64 stacks at each point. This provided sufficient spatial resolution to locate the mines. When we processed the data we set our gains to automatic gain control (AGC), did not use any time or spatial filters, and set our trace correction to the DEWOW setting. The second system we used for the land mine location with was a ThermaCAM™ SC3000. This IR-camera has a spectral range of 8-9 μm with thermal sensitivity of 0.03 °C at +30 °C and uses a quantum well infrared photon detector.

Experiment
At each of this two sites we choose a 2 meter by 2 meter study area. Inside the study areas we constructed a wooden frame with dimensions of 1 meter by 2 meter. The frame was used to house the target mines and provide a reference frame for the thermal camera and the ground penetrating radar system (Figure 2, A). The frame has removable wooden crossbeams that were used to guide the movement of the GPR. There was a centimeter scale on one of the beams that provided accuracy for the GPR step size. Two target mines were buried inside the frame area and there location was recorded. We placed an antitank mine 60 cm from the end and 50 cm from the side and an antipersonnel mine 40 cm from the end and 50 cm from the side (Figure 2, B). The antitank mine was buried at a depth of 11 cm and the antipersonnel mine was buried at a depth of 5 cm from the land surface. We also placed a third mine outside of the wooden frame, which was used to observe soil water content around the target mines. The soil water content was recorded using TDR probes that were placed around this third of 5 cm from the land surface. We also placed a third mine outside of the wooden frame, which was used to observe soil water content around the target mines. The soil water content was recorded using TDR probes that were placed around this third mine. There were 4 TDR probes placed at 3, 8, 23, and 28 cm below the surface.

Figure 2: Field area with the ground penetration radar system at a frequency of 900 MHz and IR camera (A) and geometry of antitank landmine installation (B).

For verification of the radar response model the site was irrigated with 33 cm amount of water. Before and after the water application we measured volumetric water contents with time domain reflectometry, the radar signal with the GPR, and thermal infrared images with IR-camera. The raw radar signals and IR images were analyzed using the software by Sensors & Software Ltd, Canada and ThermCAM^{TM} Researcher 2000 by FLIR Systems, respectively.

4. RESULTS AND DISCUSSION

Modeling of Radar Response

We used the Eqs. (1) - (10) to evaluate the effect of soil texture and soil water content on the radar reflection from non-metallic antitank land mine buried at a depth of 11 cm. Figure 3 shows the attenuation and reflection losses in a sand and siltloam as a function of soil water content. Soil texture has a large impact on the losses which are smallest in the sand and larger in the siltloam soil. Zero water content conditions yield acceptable radar results in both soils. Unfortunately, even a small increase of water content to 3 or 10 volume percent will immediately result in a loss of signal strength to its lowest level. The losses will decrease if the soil is wetted to a water content exceeding 15 to 30 volume percent. In the sand and the silt loam soil the losses remain quite constant at water contents exceeding 30 volume percent. It appears that watering of mine fields or waiting for the rainy season is the best strategy for mine detection in sand and silt loam soils.

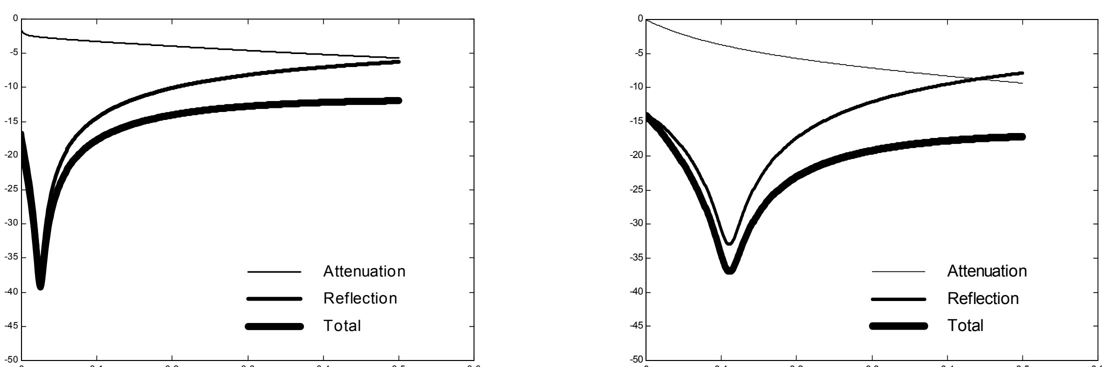

Figure 3: Attenuation and reflection losses for sand and silt loam soils for an antitank mine buried at depth of 0.11 m.

Experimental Verification of Radar Response Model
The results of the watering experiment in the Sevilleta National Wildlife Refuge are presented in Figure 4. Unfortunately, a large amount of precipitation wetted the normally dry sand soil to a volumetric water content of 7 volume percent. Nevertheless, there is a clear trend which demonstrates that the radar response improves with increasing water content from 7 to 10 to 30 volume percent in sand site and 7 to 25 to 40 in silt loam site.

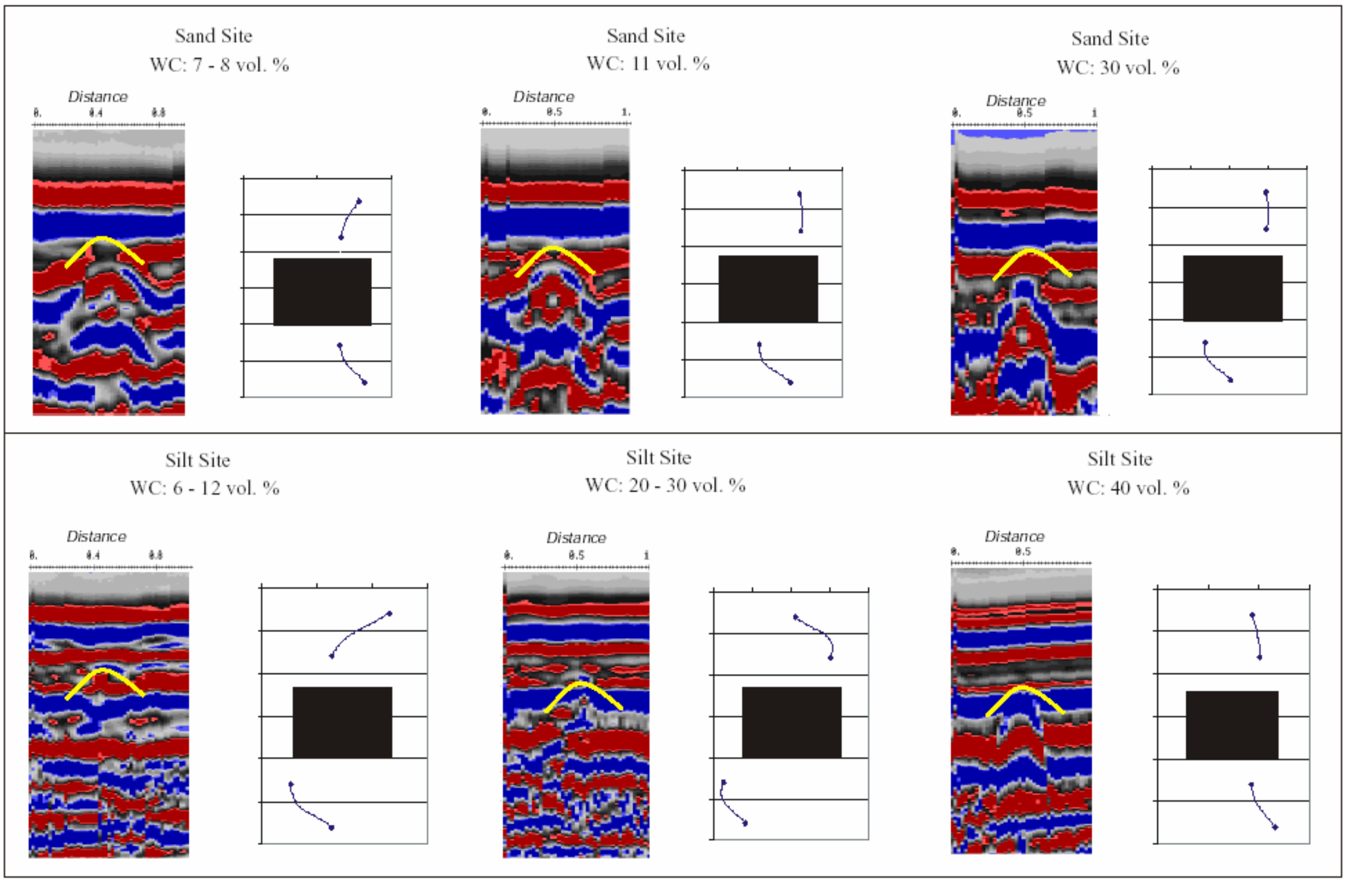

Figure 4: Radargram acquired using GPR for the various water contents (WC) in sand (above) and silt loam (below). The thick white line on the radargram is the onset of reflection from mine (left). The water content profiles have been acquired using TDR, the black box shows the antitank mine.

Thermal Infrared Images
The IR images with 7 volume percent water content (Figure 5) in the sand and silt loam sites were taken only 5 hours after mine installation. In these images, soil above the mine is whiter which indicates a cooler temperature than the surrounding area. This temperature effect is caused by the surface disturbance and is not representative for real mine fields.

The second two images were taken shortly after two days with precipitation and two weeks after mine installation. This time the mine location is darker (warmer) than the surrounding area. The last two images were obtained after saturating the sites with water, so that the area inside the frame is quite homogeneous in terms of thermal regime. Therefore, no mines are detected.

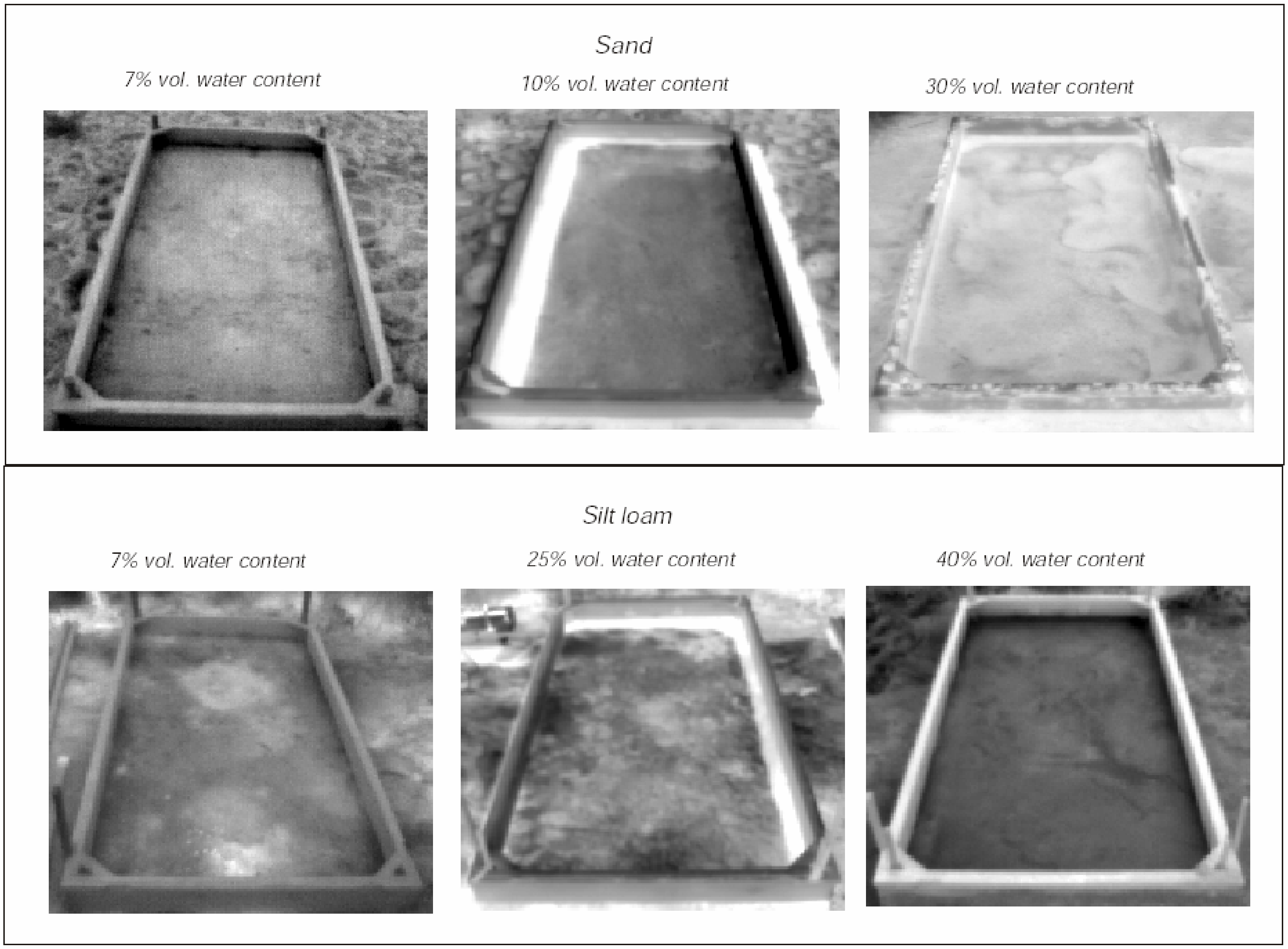

Figure 5: Thermal infrared images with different soil and water content, the top 3 figures relate to the sand and the bottom 3 figures to the silt loam.

5. CONCLUSIONS

In this study we have explored the impact of soil water content on radar and thermal signatures in a sand and silt loam soil. Our theoretical radar model predicted severe losses in the radar image at water contents between 2-10 and 5-15 volume percent in, respectively, a sand and silt loam soil. On the other hand at water contents exceeding 20 volume percent in the sand soil and 30 volume percent in the silt loam soil the losses become minimal and a good radar signature is expected (Figure 3). A qualitative assessment of the radar images obtained under field conditions (Figure 4) validates our theoretical model. In the sand soil, radar images at water contents 7-11 volume percent were marginal while at 30 volume percent a clear mine reflection was detected. In the silt loam soil, poor images were obtained at water contents 8-25 volume percent while a clear mine reflection was detected at a water content around 40 volume percent. Therefore, our theoretical model appears to work quite well for sand and silt loam soils. Since the theoretical model and our field observations have shown a clear improvement of the radar signature of a land mine at higher soil water contents, we conclude that soil watering holds promise for the enhancement of radar signatures in sand and silt loam soils.

The effect of soil water content on thermal images could not be evaluated properly due to inclement weather conditions. However, it was observed that recently placed mines may be detected by the thermal response of the disturbed surface soil.

ACKNOWLEDGMENTS

This work is funded by a grant from the Army Research Office (Project 38830-EL-LMD). The authors would like to thank Dr. Russell S. Harmon, Senior Program Manager at the Army Research Office, for his valuable advice and support.

REFERENCES

1. Das, B.S. J.M.H. Hendrickx, and B. Borchers. 2001. Modeling transient water distributions around land mines in bare soils. *Soil Science*, in press.

2. Hendrickx, J.M.H., B.S. Das, and B. Borchers. 1999. Modeling distributions of water and dielectric constants around landmines in homogeneous soils. *Detection and Remediation Technologies for Mines and Minelike Targets IV, Proceedings of SPIE*, 3710:728-738

3. Borchers, B., J.M.H. Hendrickx, B.S. Das, and S.H. Hong. 2000. Enhancing dielectric contrast between land mines and the soil environment by watering: modeling, design, and experimental results. *Detection and Remediation Technologies for Mines and Minelike Targets V, Proceedings of SPIE*, 4038:993-1000.

4. Hendrickx, J.M.H., B. Borchers, J. Woolslayer, L.W. Dekker, C. Ritsema, and S. Paton 2001. Spatial variability of dielectric properties in field soils. *Proc. of SPIE*, *This Volume*, *Detection and Remediation Technologies for Mines and Minelike Targets IV*.

5. Simunek, J., J.M.H. Hendrickx, and B. Borchers. 2001. Modeling transient temperature distributions around landmines in homogeneous bare soils. *Proc. of SPIE*, *This Volume*, *Detection and Remediation Technologies for Mines and Minelike Targets IV*.

6. DePersia, A.T., A. Bowman, P. Lucey, and E.M. Winter. 1995. Phenomenology considerations for hyperspectral mine detection. *Proceedings of SPIE*, 2496:159-167.